Hydrology and Earth System Sciences Discussions

Macropore flow of old water revisited: where does the mixing occur at the hillslope scale?

J. Klaus[1], E. Zehe[2], M. Elsner[3], C. Külls[4], and J. J. McDonnell[1]

[1]Department of Forest Engineering, Resources and Management, Oregon State University, Corvallis, OR 97331, USA
[2]Chair of Hydrology, Institute for Water Resources and River Basin Management, Karlsruher Institute of Technology KIT, Karlsruhe, Germany
[3]Helmholtz Center Munich, Munich, Germany
[4]Institute of Hydrology, Albert-Ludwigs-Universität Freiburg, Freiburg, Germany

Correspondence to: E. Zehe (erwin.zehe@kit.edu), J. Klaus (julian.klaus@oregonstate.edu)

Discussion Paper | Discussion Paper | Discussion Paper | Discussion Paper

HESSD

9, 4333–4380, 2012

Macropore flow of old water revisited at the hillslope scale?

J. Klaus et al.

Title Page

Abstract | Introduction

Conclusions | References

Tables | Figures

◄◄ | ►►

◄ | ►

Back | Close

Full Screen / Esc

Printer-friendly Version

Interactive Discussion

Abstract

The mechanisms allowing the rapid release of stored water to streams are poorly understood. Here we use a tile drained field site to combine naturally structured soils at the hillslope scale with the advantage of at least partly controlled lower boundary conditions. We performed a series of three irrigation experiments combining hydrometric measurements with stable isotope and bromide tracers to better understand macropore-matrix interactions and stored water release processes at the hillslope scale. Stable isotope concentrations were monitored in the irrigation water, the tile drain discharge and the soil water before and after the experiment. Bromide was measured at mainly every 5–15 min in the tile drain hydrograph. Different initial conditions for each experiment were used to examine how pre-event soil moisture conditions influenced flow and transport. Different amounts of irrigation water were necessary to increase tile drain discharge above the base flow level. Hydrograph separation based on bromide data revealed that irrigation water contributions to peak tile drain discharge were on the order of 20 %. Oxygen-18 and deuterium data were consistent with the bromide data and showed that pre-event soil water contributed significantly to the tile drain event flow. However, the isotopic composition of soil water converged towards the isotopic composition of irrigation water through the course of the experiment. Mixing calculations revealed that by the end of the irrigation experiments 20 % of the soil water in the entire profile was irrigation water. The isotopic data showed that the pre-event water in the tile drain was mobilized in 20–40 cm soil depth were the macropore-matrix interaction leads to an initiation of macropore flow after a moisture threshold is exceeded.

1 Introduction

Macropore flow of old water has been observed for over 20 yr now (McDonnell, 1990) but there is still much ongoing discussion whether this rapid effusion of old, pre-event

water, is indeed preferential flow or pressure wave displacement (Torres et al., 1998; Williams et al., 2002) or some combination of both. These questions lie at the heart of the double paradox, as outlined by Kirchner (2003) and tested by Bishop et al. (2004), and quantification of flow and transport processes that connect the plot, hillslope and catchment scales. Studies generally have shown that preferential flow can have a strong influence on runoff processes at the hillslope (Smettem et al., 1991; Weiler and McDonnell, 2007) and the catchment scale (Blöschl and Zehe, 2005; Zehe et al., 2007) with important controls on contaminant transport (Flury et al., 1995; Šimůnek et al., 2003). Other studies have shown that preferential flow itself can be a direct reflection of new water and dissolved substances that bypass the soil matrix and move to depth within the soil profile (Jarvis, 2007) and the amount of preferential flow is often equated to the amount of "new" water (Stone and Wilson, 2006). Beyond the issue of preferential flow vs. pressure wave release and effusion of pre-event water is the dual question of where and how mixing occurs on the event timescale: that is, where and how the event water loses its "newness". The hillslope scale is a key as this represents the scale at which plots scale processes (often very precisely defined in laboratory and column experiments) combine to yield a signature that ultimately becomes streamflow. This is a difficult problem due to the blackbox nature of subsurface mixing and, perhaps as importantly, the lack of any boundary control on quantifying such processes. Neither the early work of McDonnell (1990) nor any subsequent studies of macropore flow of old water have been able to answer this question at the hillslope scale.

So what do we know about where and how mixing occurs? Several studies have shown that flow and transport at the hillslope scale is a combination of some translatory flow (i.e., displacement) mixed with preferential flow. These ratios have been widely varying. For instance, Leaney et al. (1993) found that at the plot scale, sampled subsurface stormflow consisted mainly of storm rainfall (>90 %), that was transported via macropores bypassing the soil matrix. Vogel et al. (2008) performed a modeling study using a dual continuum approach combined with sampled oxygen-18 (^{18}O) concentrations, and found that that 24 % of the 1192 mm annual precipitation exited the

Macropore flow of old water revisited at the hillslope scale?

J. Klaus et al.

hillslope model domain as subsurface stormflow via preferential flow. Stumpp and Maloszweski (2010) used weekly ^{18}O samples in a lysimeter study to model the fraction of preferential flow in the lysimeter outflow for different cropping periods. Using a lumped parameter approach and HYDRUS 1-D, they found between 1.1 and 4.3 % preferential flow for the lumped parameter approach and 1.1 and 20.5 % for the HYDRUS 1-D approach, respectively. Kumar et al. (1997) found between 10 and 20 % preferential flow per year at a tile drained field site where the fractions were higher during intense precipitation events. In a similar study, Stone and Wilson (2006) used differences in surface water chloride concentrations and tile drain baseflow concentrations to separate tile drain discharge into a matrix and preferential flow component. Preferential flow was in total 11 and 51 % for two events while it was 40 and 81 % during peak flow.

What is clear from all of this work is that role of preferential flow is more complex than simply the transport of event water through soils or hillslope. The key question is how do preferential flow paths are interacting with their surroundings. This has been well-studied at the soil profile scale. Weiler and Naef (2003) studied the role of preferential flow during the infiltration process and the interaction between those preferential flow paths and the soil matrix. By using a dye tracer and soil profiles they found that preferential flow was initiated at the soil surface or at partially saturated soil layers. Weiler and Flühler (2004) classified water flow through soils based on dye pattern, and could distinguish between different levels of macropore-matrix interaction. Königer et al. (2010) used deutereated water to investigate flow processes in the unsaturated zone during a sprinkling experiment. They collected soil samples 12 and 35 days after irrigation and found a distinct change of deuterium (^{2}H) background towards the concentration of applied water within one meter depth. This interaction plays a crucial role in the water transported via macropores, as macropore flow depends on soil matrix infiltration capacity, interaction between macropores and matrix and connectivity of macropores (Tsuboyama et al., 1994).

Here we build upon recent work to examine hillslope scale macropore-matrix interactions. In particular, we build upon recent detailed hillslope investigations by Kienzler

Macropore flow of old water revisited at the hillslope scale?

J. Klaus et al.

Title Page

Abstract	Introduction
Conclusions	References
Tables	Figures

Back | Close

Full Screen / Esc

Printer-friendly Version

Interactive Discussion

and Naef (2008) who used ^{222}Rn to distinguish between subsurface flow supplied directly from precipitation and water displaced from saturated parts of the soil profile. We use a controlled experiment at a tile drained agricultural field site. We employ multiple tracers within a series field scale irrigation experiments to investigate flow processes through macropores, the interaction between macropores and the soil matrix, and the source of the discharging water at a tile drained field site. Our tile drained field site is effectively a hillslope scale lysimeter (Richard and Steenhuis, 1988) that allows us to address the following questions regarding macropore flow of old water:

1. What are the relative roles of pressure wave displacement versus preferential flow in the hillslope scale "macropore flow of old water"?

2. What are the interactions between macropores and the soil matrix?

3. Where does the mixing occur and how does rain amount, intensity, and duration affect this?

4. Where in the soil profile is the pre-event source water of the tile drain outflow?

2   Study site and methods

The Weiherbach valley is a nested rural catchment of 3.6 km^2 (upper catchment) and 6.3 km^2 (total) size located in a Loess area in south-west Germany. The geology is dominated by Keuper sandstone, marl and mudstone (lower and middle Triassic) and a Loess layer of up to 15 m thickness. The climate is semi-humid with an average annual precipitation of 750–800 mm, average annual runoff of 150 mm and annual potential evaporation of 775 mm. The average annual air temperature is 8.5 °C. About 95 % of the catchment area is used for agricultural purposes, 4 % is forested and 1 % is paved. Ploughing is usually to a depth of 25 cm in early spring or early autumn, but has been mainly replaced in recent years by reduced soil surface treatment (5–10 cm depth). Most of the Weiherbach hillslopes exhibit a typical Loess catena with moist but drained

Colluvisols located at the hill foot and drier Calcaric Regosols or Luvisols located at the top and mid slopes, inducing a typical distribution of preferential flow paths (Zehe and Flühler, 2001b). Earthworms such as *Lumbricus terrestris* L. play an important role in developing these preferential flow paths, which play a dominant role in water and solute
5 transport as they may reach more than one meter depth.

2.1 Experimental site and determination of soil characteristics

The irrigation experiments were performed at a field site located parallel to the Weiherbach brook (49°08′08″ N, 8°44′42″ O). This is a $20 \times 20\,\mathrm{m}^2$ plot, approximately $10\,\mathrm{m}$ from the stream banks. This field has been reused for agricultural purposes about the
10 last eight years before this study. Before that it was fallow land. A single tile drain tube is located about 1–1.2 m below the surface, embedded in a gravel layer. The tile drain outlet, a plastic tube with a diameter of approx. 20 cm, enters the Weiherbach brook about 30 cm above the baseflow water level. The soil is a Colluvisol with a strong gleyic horizon starting at a depth between 40 and 70 cm below the surface, which fits well with
15 observations of perennial flow from the tile drain.

Soil cores ($100\,\mathrm{cm}^3$) were extracted at three different locations at five depths (between 7.5 cm and 60 cm, non-uniform between the different locations) to measure soil hydraulic conductivity (constant and falling head method) and porosity. The soil hydraulic conductivity showed stratification with decreasing hydraulic conductiv-
20 ity, decreasing porosity, and increasing bulk density with depth. The hydraulic conductivities were $5.3 \times 10^{-8}\,\mathrm{m\,s}^{-1}$, $1.8 \times 10^{-8}\,\mathrm{m\,s}^{-1}$, and $1 \times 10^{-9}\,\mathrm{m\,s}^{-1}$ at 50–60 cm depth, and between $1 \times 10^{-4}\,\mathrm{m\,s}^{-1}$ and $1 \times 10^{-6}\,\mathrm{m\,s}^{-1}$ in the upper 10 cm. The soil porosity decreased from approx. 0.5 to 0.4, and the bulk density increased from approx. $1.3\,\mathrm{g\,cm}^{-3}$ to $1.7\,\mathrm{g\,cm}^{-3}$. The measured values are consistent with published soil
25 data of Delbrück (1997) and Schäfer (1999). Soil tillage of the experimental field has been annual conventional ploughing to a depth of about 25–30 cm. The experiments were performed before the annual soil tillage took place. Macropores generated by earthworms are the main factor of vertical preferential pathways in the Weiherbach

catchment (Zehe and Flühler, 2001a,b) and were counted at a horizontal soil profile in 10 cm depth after the experiments.

2.2 Experimental design of the study

Most experimental studies that perform irrigation experiments are singular events. The
idea of this study was to perform a series of repeated irrigation experiments (three in total), together with an approach that combines hydrometric measurements with tracer observations. The series was performed with slightly different initial conditions between the experiments.

2.2.1 Experimental setup

The first experiment was performed on 16 September 2008, the second on 15 September 2009, and the third three weeks later on 5 October 2009. Meteorological conditions for the weeks before the experiments were logged at a nearby met station. The irrigation was performed with a system of eight garden sprinklers (e.g., Wienhöfer et al., 2009) that were adjustable in range and received the same pressure to have the same sprinkling rate. The irrigation amount was observed and the duration and amount of the irrigation is summarized in Table 1. Soil moisture was observed during all experiment (see Sect. 3 for details). The tile drain was sealed by a plastic board with a triangular notch (opening angle was 25°) and the water level was measured during the experiment by means of a pressure probe (PD-2, Sommer, Koblach, Austria) with a temporal resolution of 1 min and 10 min after the experiments. Water levels were transformed into discharge using a rating curve that was determined by frequent discharge measurements with a bucket during the experiments. We estimate the accuracy at $0.02\,l\,s^{-1}$, which is determined by the accuracy of the pressure probe and the rating curve.

Bromide as tracer was applied during the irrigation in the first two experiments and brilliant blue during the first experiment. The isotopic signature (δ^2H and δ^{18}O) of

the irrigation water was sampled for all experiments. The breakthrough of bromide and the isotopic signature of the water were sampled at the tile drain outlet during all experiments in variable intervals. In addition we observed the soil water isotopic signature in the second experiment to determine the extent of the macropore-matrix interaction. The isotopic composition of soil water was measured in a transect (before experiment 2), from the near stream boundary of the field plot to the upper boundary. Sampling holes were closed afterwards, and the samples after the experiment were taken approx. 50 cm away from the pre-experiment samples.

2.2.2 Pre-experiment condition

As there were no continuous on-site measurements of soil moisture we report the precipitation amount for 45 days and 10 days before the experiment (Table 2). The 45 day period for the third experiment is given without the irrigation sum of the second experiment. The total potential evaporation for the pre-experimental period is also reported in Table 2, following the approach of Haude (1955) that is based on humidity and air temperature. Air temperature, humidity and precipitation (tipping bucket) were measured at a nearby met-station (700 m distance). As the first two experiments both took place in mid-September the initial conditions are comparable. The first experiment took place after a much wetter summer with more than three times the precipitation of the second experiment. Additionally, the potential evaporation, on a 45 day basis, was lower for the first experiment. Thus, the first experiment was performed in wetter conditions than the second experiment.

The macropores per square meter were counted after experiments 1 and 2 at 10 cm depth. Table 3 summarizes the number of burrows per square meter. They are classified based on their diameter, burrows or channels with a diameter below 2 mm were not included.

2.2.3 Experimental details

First experiment

The irrigation rate was measured with 10 precipitation samplers with a support of 200 cm^2 and an opening 30 cm above ground. Irrigation was carried out in three blocks of 60 min, 80 min, and 60 min duration, with 30 min breaks between the blocks. In this experiment, a tracer solution (1500 l) containing 1600 g bromide and 2000 g brilliant blue was applied during the first irrigation block on the field site (min 15 to min 35). The irrigation water had a constant isotopic signature (^{18}O = −8.1 ‰, ^{2}H = −56.1 ‰).

The day before the experiment six plastic access tubes with a diameter of 27 mm were installed vertically into the soil. They ranged from the surface to 1 m depth, without disturbing the surrounding soil matrix. These access tubes were used to measure soil moisture with a "Profile Probe – PR2" (Delta-T Devices, Burwell, UK) at six different depths (10, 20, 30, 40, 60, and 100 cm) and at six locations. These measurements were not performed continuously but only in-between the irrigation blocks.

Shortly before, during and after the experiment, water samples were taken for several tasks. Before the experiment, background concentrations of bromide, brilliant blue, ^{18}O and ^{2}H were measured in both the tile drain and the irrigation water. Irrigation water was pumped out of the nearby Weiherbach brook. During the experiment, the irrigation water was sampled three times to check whether the isotope composition remained constant. Additionally, the solute breakthrough curves were sampled by taking manual water samples at the tile drain outlet. In the beginning we sampled with a high temporal resolution of 5 min as Zehe and Flühler (2001a) reported a very fast first solute breakthrough during their experiment that was carried out at a nearby field site. Later, the sampling rate was reduced. In total we collected 51 water samples during the experimental day; the last sample was taken 2 h after the end of the experiment. Additionally, the falling limb of the hydrograph was sampled every 8 h for five days by an automatic sampler (ISCO). Six and seven days after the irrigation two additional samples were taken by hand.

Second experiment

Compared to the first experiment we improved measurements of the irrigation rate and the soil moisture measurement. Irrigation rate was measured with 20 evenly distributed precipitation samplers with a support of $37.4\,cm^2$ and approx. 5 cm above ground. Irrigation occurred in three blocks, 35 min, 90 min, and 90 min, with breaks of 22 min and 30 min. We applied 2400 g of bromide dissolved in 1500 l water with the first irrigation block (min 13 to 35). The irrigation water had a constant isotopic signature during the experiment ($^{18}O = -8.35\,‰$, $^2H = -56.0\,‰$).

To measure soil moisture continuously six Theta Probes (Delta-T Devices, Burwell, UK) were installed in a vertical soil profile at the streamside boundary of the experimental plot at depths of 10 cm, 30 cm, and 50 cm, two probes at each depth. The moisture content was logged every 5 min with the DL6 (Delta-T Devices, Burwell, UK). Additional we measured soil moisture at 20 evenly distributed locations at the field site before the experiment, between the irrigation blocks and after the experiment with a Theta Probe. We also took soil samples with a hand auger to determine the soil water isotopic composition at three locations down to a depth of approx. 60 cm before and after the experiment.

We sampled the background level of tracers in the tile drain outlet before the start of the experiment and collected a total of 25 water samples during the experiment at intervals of 15 min, the last two samples with intervals of 30 min, and three samples on the day after the experiment.

Third experiment

The irrigation rate was measured the same way as in the second experiment. Irrigation was performed in two 90 min blocks with a 30 min break between them. No artificial tracers were applied and the irrigation water had a constant isotopic composition ($^{18}O = -8.31\,‰$, $^2H = -56.1\,‰$). Unfortunately wild boars destroyed the soil moisture equipment before this experiment, so we were only able to measure surface moisture,

before the experiment, between the irrigation blocks and after the experiment. Again, tile drain background was sampled, and then 21 samples were taken during the experiment in a 15 min interval.

2.2.4 Determination of irrigation rate

Based on the 10 (1st experiment) and 20 (2nd and 3rd experiment) irrigation samplers, we evaluated the spatial correlation structure of the irrigation rates by calculating experimental variogram (Kitanidis, 1997) and fitting theoretical variogram functions. This geostatistical analysis revealed no correlation structure. Thus we used the mean value of all samplers as average irrigation rate, summarized in Table 1.

2.3 Analytics

2.3.1 Water samples

Bromide and isotopes were measured directly in filtered (450 nm) water samples. Bromide concentrations were determined by anion chromatography (ICS-1000 Dionex). Brilliant blue was analyzed with a UV-Visible spectrophotometer (UV-1601 Shimadzu) using a wave length of 630 nm. The detection limit in both cases is $0.1\,\mathrm{mg\,l^{-1}}$.

For hydrogen isotope analysis (^{2}H/^{1}H), water samples were reduced to molecular hydrogen in an uranium reactor, and the gas was subsequently introduced into the inlet of an isotope ratio mass spectrometer (Delta-S, Finnigan MAT, Germany) where it was measured against a hydrogen monitoring gas. For oxygen isotope analysis (^{18}O/^{16}O) water samples were degassed and equilibrated with CO_2 of known isotopic composition. The CO_2 was subsequently introduced into the dual inlet of an isotope ratio mass spectrometer (Delta-S, Finnigan MAT, Germany) and measured again relative to a CO_2 monitoring gas. In both cases, calibration was accomplished with three in-house standards that were calibrated against the international reference materials VSMOW, SLAP

and GISP (IAEA, Vienna). Isotope values δ^2H and δ^{18}O were expressed in parts per thousand (‰) as:

$$\delta^{18}\text{O or } \delta^2\text{H} = \left(\frac{R_{\text{Sample}}}{R_{\text{St}}} - 1\right) \times 1000$$

where R_{Sample} is the respective ^{2}H/^{1}H, or ^{18}O/^{16}O ratio, and R_{St} the Vienna-Standard Mean Ocean Water (absolute VSMOW ratio is ^{2}H/^{1}H $= 155.76 \pm 0.05 \times 10^{-6}$ and ^{18}O/^{16}O $= 2005.2 \pm 0.45 \times 10^{-6}$). The δ^2H measurements of water samples have a precision of ± 1‰, those of δ^{18}O have a precision of ± 0.1‰.

2.3.2 Analysis of soil water isotopic composition

The isotopic composition of soil water was determined using cavity ring-down laser spectrometry of water vapor equilibrated with the liquid soil water phase. Soil samples have been sealed in two nested gas-tight bags and equilibrated in a dry nitrogen atmosphere for 24 h under controlled temperature ($\pm 0.1\,^\circ$C) conditions until water-vapor phase equilibrium had been established. Based on Majoube (1971) the isotopic composition of soil water was derived from the isotopic composition of water vapor based on temperature dependent thermodynamic equilibrium fractionation. Allison et al. (1987) have demonstrated that water-vapor saturation and isotope equilibrium in the unsaturated zone prevail even in dry desert soil. Hendry et al. (2008) have used the same equilibration principle for wet clay soil and could establish water isotope profiles in deep clay. Based on parallel equilibration experiments of soil samples wetted with known liquid water isotope standards the rapid establishment of water-vapor equilibration and also of the isotope equilibration within much less than 24 h could be confirmed (C. Külls, personal communication, 2011). A mass balance of soil water compared to the total amount of vapor at saturation indicates that Rayleigh effects are far below analytical precision of 0.15–0.25‰ for δ^{18}O and of 1.0–1.5‰ for δ^2H VSMOW and do not affect the results significantly. The measurement was done using Picarro cavity ring-down

Macropore flow of old water revisited at the hillslope scale?

J. Klaus et al.

Title Page

Abstract | Introduction

Conclusions | References

Tables | Figures

◄ | ►

Back | Close

Full Screen / Esc

Printer-friendly Version

Interactive Discussion

laser spectrometry (Picarro Inc., Santa Clara, California) (Iannone et al., 2010) for water isotopes based on principles of tunable diode laser spectrometry (Gianfrani et al., 2003; Kerstel and Gianfrani, 2008; Gupta et al., 2009). Precision of measurements compared to double inlet mass spectrometer analyses is lower for δ^{18}O (0.25‰) and comparable for δ^2H (1.0‰).

2.4 Determination of event water proportion in tile drain hydrograph

To determine the fraction of irrigation water contributing to tile drain discharge during the experiment we performed a hydrograph separation based on a mass balance approach (Sklash and Farvolden, 1979). To determine the fraction of the three components in this system, i.e., tile drain baseflow, stored soil water and irrigation water, two tracers are needed. Although Lyon et al. (2009) showed a general difference in ^{18}O and ^{2}H, we could not perform a hydrograph separation between event water (irrigation) and pre-event water (baseflow and soil water) as the isotopic composition of soil water was not uniform (see section on "Isotopic composition of soil water"). Therefore we used bromide and assumed that all irrigation water will mix with the applied tracer solution. The pre-event water, i.e., soil and baseflow water, shows no background for bromide. We calculated the event water concentrations for the hydrograph separations as a time variant value $C_e(t)$ as follows:

$$C_e(t) = \frac{M_{in}(t) - M_{out}(t)}{P(t)} \tag{1}$$

where t is the experimental time in min, $M_{in}(t)$ is the bromide mass (g) that was applied on the field plot until time t, $M_{out}(t)$ is the bromide mass (g) that has left the system via the tile drain until time t, and $P(t)$ is the total irrigation amount applied on the plot until time t (liters). The hydrograph separation was then performed following Sklash and Farvolden (1979):

$$Q(t) = Q_e(t) + Q_p(t) \tag{2}$$

where $Q(t)$ is the tile drain discharge at time t, $Q_e(t)$ is the amount of irrigation water in the discharge at time t, and $Q_p(t)$ is the amount of pre-event water in the tile drain discharge at time t.

$$C(t)\, Q(t) = C_e(t)\, Q_e(t) + C_p\, Q_p(t) \qquad (3)$$

5 where $C(t)$ is the total bromide concentration $(g\,l^{-1})$ in the tile drain at time t, and C_p is the bromide concentration of the pre-event water, in this case a zero concentration.

Based on the Eqs. (2) and (3) a hydrograph separation between event and pre-event water can be performed, when the concentration of each component is known. We did this with high temporal resolution, leading to a time series over duration of the hydro-
10 graph. Additionally, the total proportion of irrigation water during the hydrograph could be calculated, and this was done until min 500 of the experiments. The hydrograph separation was done based on the measured tile drain response and the sampling during the event, and additionally we performed a hydrograph separation assuming no baseflow in the tile drain. As we did not apply bromide during the third experiment, and
15 the bromide within the soil was not evenly distributed we did not perform a hydrograph separation for this experiment.

2.5 Determination of macropore matrix interaction with isotopic data

To investigate the macropore-matrix interaction we used the measured soil water iso-topic composition of the second experiment. With this data a compartmental mixing cell
20 model was run, based on the theory of Woolhiser et al. (1982), Campana and Simp-son (1984), and Adar et al. (1988), to determine this interaction. For recent applications and methods see Klaus et al. (2008). We set up different conceptual interaction models based on the measured soil water isotopic composition and calculated the macropore-matrix interaction by mixing of event and pre-event water within the soil compartments
25 for the three sampled locations. In this study the compartments are determined by the sampling depth of the soil water isotopes and represent an undefined soil layer around those sampling depths. The analysis is based on the following assumptions:

1. The measured pre-experiment soil water isotopic composition represents the average composition of the sampled soil matrix compartment.

2. The samples taken after the experiment denote only the soil matrix isotopic composition as the macropores started to empty as the irrigation stopped. At the time of sampling (90–120 min after the experiment), the macropores were empty.

Two conceptual models of macropore matrix interaction (Fig. 1) were tested based on the isotopic data. The first model describes simple mixing of the pre-event matrix water with the irrigation water during the experiment, and the second model includes additional inflow from the soil compartment above. Calculations of the proportion between event and pre-event water were performed with ^{18}O and ^{2}H together. The first model is thus analogous to a two component hydrograph separation, with the difference that it is an over-determined system of linear equations. The second model is analogous to a three component hydrograph separation. Here, the final water composition F is composed of event water E, pre-event water P, and water entering from the upstream cell U. Based on the following three equations:

$$x_1 + x_2 + x_3 = 1 \tag{4}$$

$$x_1 C_{DE} + x_2 C_{DU} + x_3 C_{DP} = C_{DF} \tag{5}$$

$$x_1 C_{OE} + x_2 C_{OU} + x_3 C_{OP} = C_{OF} \tag{6}$$

that denote for the water mass balance (Eq. 4) (and where x_1 is the fraction of irrigation water, x_2 the fraction of water from the above soil compartment, and x_3 the fraction of water that was stored within a soil compartment before the experiment), the mass balance of ^{2}H (Eq. 5), and the mass balance of ^{18}O (Eq. 6), where C denotes the known isotopic composition while the subscripts D and O denote ^{2}H and ^{18}O, respectively, the following linear equation system can be derived:

$$\begin{pmatrix} 1 & 1 & 1 \\ C_{DE}/C_{DF} & C_{DU}/C_{DF} & C_{DP}/C_{DF} \\ C_{OE}/C_{OF} & C_{OU}/C_{OF} & C_{OP}/C_{OF} \end{pmatrix} \begin{pmatrix} x_1 \\ x_2 \\ x_3 \end{pmatrix} = \begin{pmatrix} 1 \\ 1 \\ 1 \end{pmatrix}. \tag{7}$$

Since x_1, x_2, and x_3 are constrained between 0 and 1 in Eq. (7), we used linear programming to solve the mixing problem. The error was minimized by a least squares procedure. The matrix (Eq. 7) is solved for three inflow components.

3   Results

3.1   Hydrographs, tracer breakthrough curves and soil moisture

The following results present the data of each experiment in a separate section, structured by hydrograph, tracer breakthrough, and the soil moisture data. The description of the results closes with a short summary of the main findings of each experiment.

3.1.1   Experiment 1

Hydrograph behavior

Flow in the tile drain averaged $0.11\,\mathrm{l\,s^{-1}}$ for the 30 min period before the experiment. The first irrigation block, with 12.3 mm in 80 min including the tracer solution, caused no measurable increase in discharge. During the following 30 min irrigation break, a small increase in tile drain discharge can be observed, but not clearly above uncertainty. During the second irrigation block (11.9 mm in 60 min), the tile drain discharge increased abruptly 140 min after the start of the experiment and the discharge peaked at $0.20\,\mathrm{l\,s^{-1}}$ 14 min after the end of the second irrigation block. After a short recession the discharge started to increase during the third irrigation block (9.7 mm in 80 min). The hydrograph peaked 8 min after end of irrigation at $0.37\,\mathrm{l\,s^{-1}}$. The total irrigation amount was 33.9 mm. Table 1 summarizes the irrigation blocks while Fig. 2 (left column) presents the hydrograph and tracer data of the first experiment.

Tracer breakthrough curves

Isotopic background concentrations in the tile drain were $-8.1‰$ for $\delta^{18}O$ and $-56.4‰$ for δ^2H. The field site was irrigated with water of only slightly different isotopic composition ($\delta^{18}O = -8.35‰$ and $\delta^2H = -58.5‰$). Figure 2, left column, center row, presents the temporal variation of ^{18}O and ^2H in experiment 1.

During the first irrigation block and the break between block 1 and 2 (the first 110 min), the concentration of ^{18}O fluctuated around the background value, with an average of $-8.07‰$. The moment the discharge increased the concentration of ^{18}O increased as well, and the dynamic was closely linked to discharge dynamics. The first peak in $\delta^{18}O$ ($-7.31‰$) occurred 19 min before the first discharge peak, while the second ($\delta^{18}O = -7.03‰$) occurred 7 min after the second discharge peak; please keep in mind the sampling interval of 15 min.

Deuterium concentrations behaved similarly, although the concentration for the first 110 min were higher than the background (average: $\delta^2H = -54.7‰$). The first peak also occurred 19 min before the hydrograph peak ($\delta^2H = -46.5‰$) and the second peak ($\delta^2H = -45.4‰$) 8 min before the hydrograph peak.

Note that the isotope values in the irrigation water were lower ($\delta^{18}O = -8.35‰$, $\delta^2H = -58.5‰$) than the background values in the tile drain ($\delta^{18}O = -8.1‰$, $\delta^2H = -56.4‰$). Nevertheless, $\delta^{18}O$ and δ^2H values increased with increasing tile drain discharge. One day after the irrigation, $\delta^{18}O$-values were back at the background level, while the δ^2H was slightly greater than the background.

Bromide, which labeled the irrigation water, exceeded the background concentration within 65 min after irrigation began (50 min after tracer application). Bromide concentrations are strongly correlated with the hydrograph with a coefficient of determination of $R^2 = 0.87$ at the rising limb. Bromide showed a short plateau concentration around $0.7\,\mathrm{mg\,l^{-1}}$ during the first irrigation break and then followed the dynamic of the hydrograph, with two peaks at concentrations of $9.18\,\mathrm{mg\,l^{-1}}$ and $15.41\,\mathrm{mg\,l^{-1}}$ (280 min). The

additional applied brilliant blue showed a similar behavior with lower concentrations, due to sorption.

Soil moisture observations

The installation of the access tube, just the day before the experiment, limits the quality of the soil moisture data, since the contact between the plastic tube and the soil was limited. The absolute measured moisture values are too high, considering that maximum measured porosity was at 54 % and that only in the loose topsoil. Before the experiment, soil moisture was stratified, with drier conditions in the upper 30 cm, and higher moisture at 60 cm and 100 cm depth. Soil moisture at 10 cm depth reached its maximum at four of six measuring location after the first irrigation block, and remained constant throughout the day. At the two other soil moisture stations maximum was reached after the second and third block, respectively. The soil moisture at 20 cm depth increased slightly until experimental min 200 and then stayed constant or decreased.

Main findings in the first experiment

Based on the combination of the different experimental approaches we summarize the experimental results. An increase in tile drain discharge did not begin directly after the start of the irrigation, but during the second irrigation block, and was then strongly linked to the irrigation pattern. At times when no clear change in isotopic composition of tile drain discharge was measurable, we did neither observe bromide nor brilliant blue in the tile drain discharge. At the moment when discharge clearly increased, bromide, brilliant blue, ^{18}O, and ^{2}H concentrations increased. The change in isotopic composition points to an activation of an additional water source: soil water.

3.1.2 Experiment 2

Hydrograph behavior

The tile drain showed an average discharge of $0.10\,l\,s^{-1}$ for the 30 min before the experiment. During the first irrigation block (5.3 mm in 35 min) the tile drain discharge showed no measurable response. A significant increase in discharge began after 105 min after onset of the experiment, leading to a double peaked hydrograph. The first peak ($0.16\,l\,s^{-1}$) occurred 164 min after the experiment started and the second peak ($0.31\,l\,s^{-1}$) at min 276, 8 min after the end of irrigation. Figure 2 (center column) shows the hydrograph and the irrigation blocks, while precipitation amount is given in Table 1. The total irrigation sum was 41.1 mm.

Tracer breakthrough curves and soil water isotopes

Background δ^{18}O and δ^{2}H values in the tile drain were -8.0‰ and -57.5‰, respectively. The irrigation water had an isotopic composition of δ^{18}O $= -8.3$‰ and δ^{2}H $= -56$‰. Figure 2 (center column, center plot) presents the temporal variation of ^{18}O and ^{2}H in experiment 2.

The average δ^{18}O value during the first irrigation block was -8‰. Near the time of the first hydrograph peak water δ^{18}O was -7.6‰ and during the second peak the value was -7.3‰. The fluctuations in ^{18}O were more erratic during the second experiment than during the first experiment and in general were more erratic than those of ^{2}H. Deuterium (Fig. 2, center column, center plot) showed nearly continuous increases and peaked 4 min after discharge at δ^{2}H $= -50.4$‰. The δ^{18}O-values the day after the experiment were at background levels, as were those of deuterium.

Similar to the first experiment the isotopic signature of the tile drain discharge increased during the experiment relative to the irrigation and background water. In this experiment this changed can be clearly associated with the observed isotopic signature of the soil water. The isotopic composition of soil water was measured before and

after the experiment and the data is presented in Fig. 3, the left column presents the [18]O values and the right column the deuterium values. To repeat: the isotopic composition of irrigation water was $\delta^{18}O = -8.3\,‰$ and $\delta^2H = -56\,‰$. The pre-experiment isotopic composition of soil water showed a decrease in the δ-values for both isotopes with depth. This stratification is frequently observed in soil water studies (Allison et al., 1993; Barnes and Walker, 1989; Königer et al., 2010) and results from evaporation.

After the irrigation experiment, the isotopic composition of soil water moved towards the composition of the irrigation water. The stratification with depth was conserved, indicating mixing with existing soil water and not full replacement of soil water by irrigation water. Both isotopes, [18]O and ^{2}H, showed the same mixing process between soil water and irrigation water in the sampled soil profiles

The bromide concentrations exceeded the background value after 100 min, which occurred shortly before the increase in discharge. Bromide concentrations are strongly correlated with the hydrograph with a coefficient of determination of 0.9 at the rising limb. Bromide concentration peaked at 10.1 mg l^{-1} (min 160) and at 16.8 mg l^{-1} (min 276), near the times of peak discharge. The concentration was decreasing slightly after the end of the irrigation. The day after the experiment (not shown in Fig. 2), concentrations were still above background.

Soil moisture observation

Surface soil moisture, measured during the irrigation breaks at the precipitation samplers, shows mainly uniform behavior. At the beginning measured surface soil moisture was between 18.5 % and 35 %, with an average of 28 % and a standard deviation of 4 %. Then soil moisture increased towards saturation reaching average values of 36.7 % (standard deviation: 4.5 %), 39.7 % (4 %) and 43.5 % (5.1 %) after the end of each irrigation block. Surface water ponding occurred at depressions at the end of the first irrigation block, and became widespread during the second irrigation block. Soil moisture as a function of depth was measured at the stream side boundary of the experimental plot. Those parts of the plot received less irrigation then average, and only

minor ponding occurred at this location. Figure 4 summarizes the moisture dynamics during the experiment. The most rapid and strongest changes in soil moisture were measured at 10 cm depth, soil moisture at greater depths showed only small changes, remaining unsaturated throughout the experiment.

5 **Main findings in the second experiment**

Again tile drain discharge started to increase during the second irrigation block. It seems that a certain amount of cumulated irrigation is needed to activate subsurface water flows. After activation, the irrigation pattern and the hydrograph are again tightly linked. Isotope values increased until peak discharge was reached, becoming more 10 distinct compared to tile drain background and irrigation water. The data from the soil water isotopic composition proofed the mobilization of soil water. Bromide concentrations slightly exceeded background values before discharge increased.

3.1.3 Experiment 3

Hydrograph behavior

15 Pre-experiment water level and discharge were lowest for the third experiment ($0.09 \, \mathrm{l \, s^{-1}}$) compared to the others (Fig. 2, right column). Although discharge appeared to increase slightly during the first irrigation block (18.1 mm in 90 min); this change was within the range of observation accuracy. Approximately 180 min after the start of the irrigation, during the second irrigation block (21.8 mm in 90 min), discharge increased 20 clearly and peaked 230 min after the start of the experiment ($0.19 \, \mathrm{l \, s^{-1}}$). After the peak, discharge decreased and reached the pre-event level about 300 min later. The total irrigation amount (Table 1) was 39.9 mm.

Tracer breakthrough curve

During the first 180 min of the experiment, the measured [18]O was not significant different than the background value of −8‰. The ^{18}O-value in irrigation water (−8.3‰) was more negative than the background value. With the increase in tile drain discharge δ^{18}O-values increased markedly. The peak concentration of δ^{18}O = −7.6‰ was reached 255 min after the irrigation started.

There were no clear trends in the δ^2H values. The samples varied around a value of −55.0‰ with a maximum of −51.9‰ and a minimum of −57.8‰ and no clear temporal pattern. The trends in δ^{18}O values indicate an additional source of water that contributed to the tile drain discharge during the experiment, but this cannot be confirmed by the patterns in δ^2H values.

Background bromide concentrations in tile drain baseflow were below the detection limit, indicating no or very limited connectivity of the soils to the tile drain. Considerable amounts of bromide must been stored in the soil from the previous experiment. During the irrigation no bromide was added to the system. Bromide was first detected (0.57 mg l^{-1}) 105 min after the irrigation began. Coincident with the increase of δ^{18}O-values, bromide concentrations also increased clearly and peaked 225 min after the experimental start at a value of 7.48 mg l^{-1}. The contribution of bromide indicates a contribution from soil water.

Soil moisture observation

Surface moisture, measured before the experiment and after the irrigation blocks, showed a strong increase. Some measured locations showed no significant difference after the first and second irrigation block, indicating that saturation was reached after one irrigation block. Average surface soil moisture was 26.8 % before the experiment, with a standard deviation of 5.3 %, reached 42.8 % after the first irrigation block (SD = 2.7 %) and 44.9 % after the second block (SD = 3.3 %).

Main findings of the third experiment

In summary, bromide that must have been previously stored in the soil matrix, was remobilized during the experiment, and was exported by the tile drain, underlining the observation based on the water isotopes. The time at which soil water began to contribute is clearer for bromide than for the isotopes. Nevertheless, the soils within the system showed no contribution to tile drain discharge at the beginning of the experiment, but the irrigation led to significant contributions of soil water.

3.2 Hydrograph separation to distinguish between irrigation water and pre-event water

In this section we evaluate the proportion of irrigation water in the tile drain hydrograph. Figure 5 presents the results for the first two experiments. During the first experiment, the maximum proportion of irrigation/event water was 13.2 % after 280 min, corresponding to the highest bromide concentrations. The proportion of event water follows the double peak shape of the hydrograph and the bromide concentrations. In total 5 % of the tile drain discharge in the first 500 min of the experiment was irrigation water (12 % without baseflow). Evaluating the hydrograph only for the water that was mobilized within the experiment, the maximum proportion was 19.5 % and the proportion of event water during both hydrograph peaks was similar.

The temporal pattern of event water fractions during the second experiment was similar to the corresponding one of the first experiment. The maximum proportions were slightly smaller with 11.6 % (with baseflow) and 18 % (without baseflow) compared to the first experiment, while the total proportion of event water was 6.2 % (13 % without baseflow), slightly higher. This latter observation resulted from the different shape of the declining hydrograph. In summary, the event water proportion showed high temporal variability during both experiments, and even when assuming no baseflow, the total event-water proportion never exceeded 20 %. The pre-event water, as indicated by the isotope data was mobilized soil water. At times when discharge was not distinctly

different from baseflow, we did not calculate the percentage of event water because since we would have to divide by very small numbers.

3.3 Compartmental modeling

We performed compartmental mixing modeling to investigate the interaction between the macropore system and the soil matrix. So, what is the amount of water that entered the soil matrix compartment? We evaluated this interaction for every sampling location, to account for the spatial variability within the experimental plot that derived from variable soil structure.

Table 4 summarizes the results of the compartmental modeling. The results based on two end members (pre-event soil matrix water and irrigation water) indicate a clear interaction between soil matrix and the irrigation water over the depth of the profile. For example, at sampling location 1, the matrix water after the experiment consisted of 10.0 % to 34.1 % irrigation water, depending on the depth. The results for location 2 and 3 are similar (Table 4). Using water from the overlying soil compartment as an additional end member, led to somewhat different results. Mainly location 3 showed contributions of water from overlying soil layers while this is not pronounced for location 1 and 2.

With the applied linear programming, the sum of the individual errors of each mass balance equation (row in the matrix of Eq. 7) is minimized. The mass balance error for each individual mass balance (water, ^{18}O and ^{2}H) showed a maximum deviation of -6.2 %. In total 71.6 % of the individual mass balance errors are below ± 2 %. Approaches allowing water from compartment 2 to enter compartment 4 were not allowed during the modeling, as this would have led to an underdetermined linear equation system, and thus a non-unique result.

3.4 Backward determination of isotopic composition of soil water contributing to the hydrograph

The hydrograph separation approach can be solved in a backward approach to determine the isotopic signature of contributing soil water. Using Eqs. (3) and (4) with three components, namely irrigation water, soil water, and baseflow, we can determine the isotopic composition of soil water contributing to the hydrograph. The fraction of base flow contribution was calculated by the ratio of baseflow (assumed to be constant) to measured flow, and the fraction of soil water was calculated as residual.

Figure 6 presents the isotopic composition of contributing soil water. Combined with Fig. 3, we can infer on the soil layer that contributed water to the hydrograph. Unfortunately ^{18}O and ^{2}H provide different results. The calculated soil water signature of δ^{18}O-values varies around $-6.5\,‰$ during the times of clear discharge increase while δ^{2}H-values are around $-44\,‰$. While ^{18}O would indicate a contribution of soil water from depths between 20 cm and 40 cm, ^{2}H results would indicate contributing soil layer at approx. 20 cm. This calculation is very sensitive to (a) measured discharge, (b) calculated fraction of event water, and (c) measured concentration, which can explain the discrepancy. For example, an assumed baseflow of $0.08\,\mathrm{l\,s^{-1}}$ compared to the measured $0.10\,\mathrm{l\,s^{-1}}$ would change the δ^{2}H-values around peakflow from $-46\,‰$ to $-47\,‰$. Additionally, the spatial variation in isotopic composition of soil water can be higher than sampled by three profiles.

4 Discussion

4.1 Macropore flow of old water re-defined

Macropore flow of old water is really a euphemism for a complex range of water mixing issues that occur from plot scale vertical infiltration to lateral flow at the hillslope scale. Key among them is the relative roles of pressure wave displacement versus preferential

Title Page

Abstract | Introduction

Conclusions | References

Tables | Figures

|◄ | ►|

◄ | ►

Back | Close

Full Screen / Esc

Printer-friendly Version

Interactive Discussion

CC BY

flow in resultant hillslope-scale flow initiation and the interactions between macropores and the soil matrix. These processes are at the heart of grand challenges in the field of hillslope hydrology and questions of where does mixing occur and how and where is the pre-event source water mobilized? With the sprinkler experiments we were able to show that pre-event water from a soil depth of 20–40 cm entered the preferential flow paths and mixed with the irrigation water. Our work is consistent with the findings of old water generation in subsurface flow at the hillslope scale (Kienzler and Naef, 2008) and shows that a distinct soil layer contributes the pre-event water at this field site with a structured soil in the Weiherbach valley. Figure 7 presents the conceptual vertical flow model in the field soil and the two main flow processes at the beginning and during the high flow phase determined for experiment 2.

We were able to constrain our perceptual model with observations of soil water isotopic composition and its change in response to the irrigation. A compartmental mixing model allowed us to quantify the extent of this interaction over the depth of the soil profile. A clear proportion of event water entered the soil matrix domain over a depth down to 60 cm consistent with vertical preferential flow of storm rainfall (Flury, 1996; Zehe and Flühler, 2001a; Weiler and Naef, 2003; Van Schaik et al., 2008) Our isotope- and bromide-based hydrograph separations showed that soil water contributions exceeded 50 % of flow during the discharge peak. This soil water contribution was activated after exceedance of a capacity threshold controlled by initial soil moisture and amount of rainfall, consistent with other recent threshold observations in hillslope activation (Tromp-van Meerveld and McDonnell, 2006a,b; Zehe et al., 2007; Zehe and Sivapalan, 2009). We observed that below the threshold, macropores drained into the matrix. After exceeding this threshold, the matrix began to drain into the macropore system, contributing then directly to the delivery the old water. This resulted in increased bromide concentrations in the tile drain and a resulting isotopic composition that strongly deviated from that of baseflow and irrigation water (Fig. 7).

4.2   Translatory flow and pressure wave evidence?

We found no evidence of translatory flow or pressure wave effects on the event timescale. Peaks in water flow and bromide transport occurred at the same time. Similarly, the change in the shape of the soil water isotopic profile (Fig. 3) showed no evidence of matrix displacement. These findings are contrary to concepts of translatory flow (Horton and Hawkins, 1965; Hewlett and Hibbert, 1967) or transport by pressure waves (Torres et al., 1998; Williams et al., 2002) that have been used to explain the rapid transport of old water in some systems. In our study, translatory flow would have led to a downward propagation of a distinct isotopic signature, whereas our results indicate a strong mixing of irrigation water and pre-event soil water in the profile.

Figure 8 illustrates the mixing dynamics during experiments 1 and 2. In both experiments the isotopic composition of the tile drain flow was similar before and after the experiments. During the hydrograph, soil water contributed to the hydrograph and led to different signatures during rise and fall of the hydrograph. Figure 8 gives an insight to the temporal development of source regions and source fractions.

4.3   A solely vertical process or lateral contributions to flow?

The direct contribution of vertical macropores to tile drain discharge is usually limited in distance to the tile drain. Shipitalo and Gibbs (2000) found that macropores up to a distance of 50 cm to a tile drain are directly connected to it.

With such a small area above the tile drain, the total mass recovery of bromide (6.1 %) and water (15 %) (Experiment 2) could not be explained. Assuming that all applied bromide reaches a depth of 1–1.2 m (depth of tile drain), a total recovery of 6.1 % bromide would need a contributing area of 1.2 m above the drain. Since a significant amount of bromide was stored in the soil after application (data not shown) more contributing area is needed, so that vertical contribution cannot fully explain the recovery. In a tile drain modeling study in the same catchment Klaus and Zehe (2010) showed

that a hillslope contributing width of 2–3 m at a tile drained site is needed to fit the discharge of an irrigation experiment with a 2-D hillslope model. This was also found to be consistent with the solute transport (Klaus and Zehe, 2011). Thus more than vertical transport is reasonable. Transport by pressure propagation can be neglected in this experiment, as most bromide arrived during the peak discharge and most water sourced upper soil layers (see above). We observed a temporal water table at depths of 28 cm and 40 cm after the experiment at locations 1 and 2, without an throughout saturation of the soil, so a shallow groundwater table is unlikely the reason for the lateral transport. Thus we suggest that a network of saturated pores caused additional transport of water and solutes towards the tile drain. A similar process was observed by Van Schaik et al. (2008), who found lateral preferential flow in a hillslope pore network with a temporal water table, while the soil matrix remained largely unsaturated.

4.4 On the importance of our findings for catchment-scale hydrograph separation studies

Our work has important implications for isotope-based hydrograph separations at the catchment scale. Such hydrograph separations are based on the assumption that soil water does not contribute to the storm hydrograph or that its composition is similar to that of groundwater (Sklash and Farvolden, 1979). Clearly this is not the case and the additional activation of vadose zone water can invalid this assumption (DeWalle et al., 1988). There have been numerous studies that have shown two component source fractions exceeding 100 % (e.g., Swistock et al., 1989) and several studies have shown the importance of vadose zone contributions to storm runoff by sampling the soil water end member and quantifying its effect on the hydrograph composition in the context of hydrograph separation (Kennedy et al., 1986; Swistock et al., 1989; Bazemore et al., 1994; Kendall et al., 2001). What no studies to date have been able to do, is quantify mechanistically, the relevant processes that lead to the rapid mobilization of vadose zone waters that then contribute to streamflow generation. Our work shows that activation of soil water can occur during the events and that these contributions

can be the major source of the hydrograph composition. Our findings suggest then, that also the spatial variability of soil water must be considered on catchment scale both in depth and in the area. If hydrological connectivity increases during an event a progressively greater soil volume contributes to subsurface runoff and catchment discharge. Thus, a variable source soil volume approach is needed to describe pre-event water at catchments (e.g., Harris et al., 1995), analogous to the variable source area concept used to describe the catchment runoff process (Hewlett and Hibbert, 1967; Dunne and Black, 1970).

5   Conclusions

We employed multiple tracers within a series field scale irrigation experiments to investigate flow processes through macropores, the interaction between macropores and the soil matrix, and the source of the discharging water at a tile drained field site. We found that water transport through soil was governed by macropore flow and that macropore flow was itself a mixture of event and pre-event water. Pre-event water dominated the storm hydrograph on this field site with vertical preferential flowpaths. The flow mechanisms were driven by the interaction between the soil matrix and the macropore network. Our measurement of soil water isotopic composition in combination with compartmental modeling allowed us to quantify the magnitude of macropore-matrix interaction. We found that up to 30 % of soil water was derived from the irrigation. Combination of soil water isotope measurement, hydrograph separation based on applied bromide, and a backward hydrograph separation to determine the necessary isotopic signature of the soil water, allowed is to pinpoint the active soil layers that generated tile drain discharge. These layers extended from 20–40 cm depth below the soil surface.

Macropore flow of old water revisited at the hillslope scale?

J. Klaus et al.

Title Page

Abstract	Introduction
Conclusions	References
Tables	Figures

◀◀   ▶▶

◀   ▶

Back   Close

Full Screen / Esc

Printer-friendly Version

Interactive Discussion

References

Adar, E. M., Neuman, S. P., and Woolhiser, D. A.: Estimation of spatial recharge distribution using environmental isotopes and hydrochemical data, I. Mathematical model and application to synthetic data, J. Hydrol., 97, 251–277, 1988.

Allison, G. B., Colin-Kaczala, C., Filly, A., and Fontes, J. C.: Measurement of isotopic equilibrium between water, water vapour and soil CO_2 in arid zone soils, J. Hydrol., 95, 131–141, 1987.

Barnes, C. J. and Walker, G. R.: The distribution of deuterium and oxygen-18 during unsteady evaporation from a dry soil, J. Hydrol., 112, 55–67, 1989.

Bazemore, D. E., Eshleman, K. N., and Hollenbeck, K. J.: The role of soil water in stormflow generation in a forested headwater catchment: synthesis of natural tracer and hydrometric evidence, J. Hydrol., 162, 47–75, 1994.

Bishop, K., Seibert, J., Köhler, S., and Laudon, H.: Resolving the Double Paradox of rapidly mobilized old water with highly variable responses in runoff chemistry, Hydrol. Process., 18, 185–189, doi:10.1002/hyp.5209, 2004.

Blöschl, G. and Zehe, E.: On hydrological predictability, Hydrol. Process., 19, 3923–3929, 2005.

Campana, M. E. and Simpson, E. S.: Groundwater residence times and recharge rates using a discrete-state compartment model and ^{14}C data, J. Hydrol., 72, 171–185, 1984.

Delbrück, M.: Großflächiges Bromid-Tracerexperiment zur räumlichen und zeitlichen Variabilität des Wassertransports an einem Lößhang, Naturwissenschaftlich-Mathematische Gesamtfakultät, Ruprecht-Karls-University of Heidelberg, Heidelberg, Germany, 1997.

DeWalle, D. R., Swistock, B. R., and Sharpe, W. E.: Three-component tracer model for stormflow on a small Appalachian forested catchment, J. Hydrol., 104, 301–310, 1988.

Dunne, T. and Black, R.: Partial Area Contributions to Storm Runoff in a Small New England Watershed, Water Resour. Res., 6, 1296–1311, 1970.

Flury, M.: Experimental Evidence of Transport of Pesticides through Field Soils-a review, J. Environ. Qual., 25, 25–45, doi:10.2134/jeq1996.00472425002500010005x, 1996.

Flury, M., Leuenberger, J., Studer, B., and Flühler, H.: Transport of anions and herbicides in a loamy and a sandy field soil, Water Resour. Res., 31, 823–835, 1995.

Gianfrani, L., Gagliardi, G., van Burgel, M., and Kerstel, E.: Isotope analysis of water by means of near infrared dual-wavelength diode laser spectroscopy, Opt. Express, 11, 1566–1576, 2003.

Gupta, P., Noone, D., Galewsky, J., Sweeney, C., and Vaughn, B. H.: A new laser-based, field-deployable analyzer for laboratory-class stable isotope measurements in water, Geochima. Cosmochim. Acta, 73, A480–A480, 2009.

Harris, D. M., McDonnell, J. J., and Rodhe, A.: Hydrograph Separation Using Continuous Open System Isotope Mixing, Water Resour. Res., 31, 157–171, doi:10.1029/94wr01966, 1995.

Haude, W.: Zur Bestimmung der Verdunstung auf möglichst einfache Weise, Mitt. Dt. Wetterd., 2, Bad Kissingen, 1955.

Hendry, M. J., Wassenaar, L. I., and Lis, G. P.: Stable isotope composition of gaseous and dissolved oxygen in the subsurface, Geochim. Cosmochim. Acta, 72, A367, 2008.

Hewlett, J. D. and Hibbert, A. R.: Factors affecting the response of small watersheds to precipitation in humid areas, in: Forest Hydrology, edited by: Sopper, W. E. and Lull, H. W., Pergamon Press, New York, 275–290, 1967.

Horton, J. H. and Hawkins, R. H.: Flow path of rain from the soil surface to the water table, Soil Sci., 100, 377–383, 1965.

Iannone, R. Q., Romanini, D., Cattani, O., Meijer, H. A. J., and Kerstel, E. R. T.: Water isotope ratio (δ^2H and δ^{18}O) measurements in atmospheric moisture using an optical feedback cavity enhanced absorption laser spectrometer, J. Geophys. Res., 115, D10111, doi:10.1029/2009jd012895, 2010.

Jarvis, N. J.: A review of non-equilibrium water flow and solute transport in soil macropores: principles, controlling factors and consequences for water quality, Eur. J. Soil Sci., 58, 523–546, doi:10.1111/j.1365-2389.2007.00915.x, 2007.

Kendall, C., McDonnell, J. J., and Gu, W.: A look inside 'black box' hydrograph separation models: a study at the Hydrohill catchment, Hydrol. Process., 15, 1877–1902, doi:10.1002/hyp.245, 2001.

Macropore flow of old water revisited at the hillslope scale?

J. Klaus et al.

Kennedy, V. C., Kendall, C., Zellweger, G. W., Wyerman, T. A., and Avanzino, R. J.: Determination of the components of stormflow using water chemistry and environmental isotopes, Mattole River basin, California, J. Hydrol., 84, 107–140, 1986.

Kerstel, E. and Gianfrani, L.: Advances in laser-based isotope ratio measurements: selected applications, Appl. Phys. B-Lasers O., 92, 439–449, doi:10.1007/s00340-008-3128-x, 2008.

Kienzler, P. M. and Naef, F.: Subsurface storm flow formation at different hillslopes and implications for the "old water paradox", Hydrol. Process., 22, 104–116, doi:10.1002/hyp.6687, 2008.

Kirchner, J. W.: A double paradox in catchment hydrology and geochemistry, Hydrol. Process., 17, 871–874, doi:10.1002/hyp.5108, 2003.

Kitanidis, P. K.: Introduction to Geostatistics: Applications in Hydrogeology, Cambridge University Press, Cambridge, UK, 271 pp., 1997.

Klaus, J. and Zehe, E.: Modelling rapid flow response of a tile-drained field site using a 2D physically based model: assessment of "equifinal" model setups, Hydrol. Process., 24, 1595–1609, doi:10.1002/hyp.7687, 2010.

Klaus, J. and Zehe, E.: A novel explicit approach to model bromide and pesticide transport in connected soil structures, Hydrol. Earth Syst. Sci., 15, 2127–2144, doi:10.5194/hess-15-2127-2011, 2011.

Klaus, J., Külls, C., and Dahan, O.: Evaluating the recharge mechanism of the Lower Kuiseb Dune area using mixing cell modeling and residence time data, J. Hydrol., 358, 304–316, 2008.

Königer, P., Leibundgut, C., Link, T., and Marshall, J. D.: Stable isotopes applied as water tracers in column and field studies, Org. Geochem., 41, 31–40, 2010.

Kumar, A., Kanwar, R. S., and Hallberg, G. R.: Separating preferential and matrix flows using subsurface tile flow data, J. Environ Sci. Heal. A, 32, 1711–1729, 1997.

Leaney, F. W., Smettem, K. R. J., and Chittleborough, D. J.: Estimating the contribution of preferential flow to subsurface runoff from a hillslope using deuterium and chloride, J. Hydrol., 147, 83–103, 1993.

Lyon, S. W., Desilets, S. L. E., and Troch, P. A.: A tale of two isotopes: differences in hydrograph separation for a runoff event when using δD versus δ^{18}O, Hydrol. Process., 23, 2095–2101, doi:10.1002/hyp.7326, 2009.

Majoube, M.: Fractionnement en oxygène-18 et en deuterium entre l'eau et sa vapeur, J. Chim. Phys., 197, 1423–1436, 1971.

Title Page

Abstract | Introduction

Conclusions | References

Tables | Figures

|◄ | ►|

◄ | ►

Back | Close

Full Screen / Esc

Printer-friendly Version

Interactive Discussion

McDonnell, J. J.: A rationale for old water Discharge Through Macropores in a Steep, Humid Catchment, Water Resour. Res., 26, 2821–2832, 1990.

Richard, T. L. and Steenhuis, T. S.: Tile drain sampling of preferential flow on a field scale, J. Contam. Hydrol., 3, 307–325, 1988.

Schäfer, D.: Bodenhydraulische Eigenschaften eines Kleineinzugsgebiets – Vergleich und Bewertung unterschiedlicher Verfahren, University of Karlsruhe, Karlsruhe, Germany, 1999.

Shipitalo, M. J. and Gibbs, F.: Potential of Earthworm Burrows to Transmit Injected Animal Wastes to Tile Drains, Soil Sci. Soc. Am. J., 64, 2103–2109, doi:10.2136/sssaj2000.6462103x, 2000.

Šimůnek, J., Jarvis, N. J., v. Genuchten, M. T., and Gaerdenaes, A.: Review and comparison of models for describing non-equilibrium and preferential flow and transport in the vadose zone, J. Hydrol., 272, 14–35, 2003.

Sklash, M. G. and Farvolden, R. N.: The role of groundwater in storm runoff, J. Hydrol., 43, 45–65, 1979.

Smettem, K. R. J., Chittleborough, D. J., Richards, B. G., and Leaney, F. W.: The influence of macropores on runoff generation from a hillslope soil with a contrasting textural class, J. Hydrol., 122, 235–251, 1991.

Stone, W. W. and Wilson, J. T.: Preferential Flow Estimates to an Agricultural Tile Drain with Implications for Glyphosate Transport, J. Environ. Qual., 35, 1825–1835, doi:10.2134/jeq2006.0068, 2006.

Stumpp, C. and Maloszewski, P.: Quantification of preferential flow and flow heterogeneities in an unsaturated soil planted with different crops using the environmental isotope δ^{18}O, J. Hydrol., 394, 407–415, 2010.

Swistock, B., DeWalle, D., and Sharpe, W.: Sources of Acidic Storm Flow in an Appalachian Headwater Stream, Water Resour. Res., 25, 2139–2147, 1989.

Torres, R., Dietrich, W. E., Montgomery, D. R., Anderson, S. P., and Loague, K.: Unsaturated zone processes and the hydrologic response of a steep, unchanneled catchment, Water Resour. Res., 34, 1865–1879, doi:10.1029/98wr01140, 1998.

Tromp-van Meerveld, H. J. and McDonnell, J. J.: Threshold relations in subsurface stormflow: 1. A 147-storm analysis of the Panola hillslope, Water Resour. Res., 42, W02410, doi:10.1029/2004wr003778, 2006a.

Macropore flow of old water revisited at the hillslope scale?

J. Klaus et al.

Title Page

Abstract | Introduction

Conclusions | References

Tables | Figures

◄◄ | ►►

◄ | ►

Back | Close

Full Screen / Esc

Printer-friendly Version

Interactive Discussion

Tromp-van Meerveld, H. J. and McDonnell, J. J.: Threshold relations in subsurface stormflow: 2. The fill and spill hypothesis, Water Resour. Res., 42, W02411, doi:10.1029/2004wr003800, 2006b.

Tsuboyama, Y., Sidle, R. C., Noguchi, S., and Hosoda, I.: Flow and solute transport through the soil matrix and macropores of a hillslope segment, Water Resour. Res., 30, 879–890, doi:10.1029/93wr03245, 1994.

Van Schaik, N. L. M. B., Schnabel, S., and Jetten, V. G.: The influence of preferential flow on hillslope hydrology in a semi-arid watershed (in the Spanish Dehesas), Hydrol. Process., 22, 3844–3855, doi:10.1002/hyp.6998, 2008.

Vogel, T., Sanda, M., Dusek, J., Dohnal, M., and Votrubova, J.: Using Oxygen-18 to Study the Role of Preferential Flow in the Formation of Hillslope Runoff, Vadose Zone J., 9, 252–259, doi:10.2136/vzj2009.0066, 2008.

Weiler, M. and Flühler, H.: Inferring flow types from dye patterns in macroporous soils, Geoderma, 120, 137–153, 2004.

Weiler, M. and McDonnell, J. J.: Conceptualizing lateral preferential flow and flow networks and simulating the effects on gauged and ungauged hillslopes, Water Resour. Res., 43, W03403, doi:10.1029/2006wr004867, 2007.

Weiler, M. and Naef, F.: An experimental tracer study of the role of macropores in infiltration in grassland soils, Hydrol. Process., 17, 477–493, 2003.

Wienhöfer, J., Germer, K., Lindenmaier, F., Färber, A., and Zehe, E.: Applied tracers for the observation of subsurface stormflow at the hillslope scale, Hydrol. Earth Syst. Sci., 13, 1145–1161, doi:10.5194/hess-13-1145-2009, 2009.

Williams, A. G., Dowd, J. F., and Meyles, E. W.: A new interpretation of kinematic stormflow generation, Hydrol. Process., 16, 2791–2803, doi:10.1002/hyp.1071, 2002.

Woolhiser, D. A., Gardner, H. R., and Olsen, S. R.: Estimation of multiple inflows to a stream reach using water chemistry data, Trans. ASAE, 25, 616–626, 1982.

Zehe, E. and Flühler, H.: Preferential transport of isoproturon at a plot scale and a field scale tile-drained site, J. Hydrol., 247, 100–115, 2001a.

Zehe, E. and Flühler, H.: Slope scale variation of flow patterns in soil profiles, J. Hydrol., 247, 116–132, 2001b.

Zehe, E. and Sivapalan, M.: Threshold behaviour in hydrological systems as (human) geo-ecosystems: manifestations, controls, implications, Hydrol. Earth Syst. Sci., 13, 1273–1297, doi:10.5194/hess-13-1273-2009, 2009.

Macropore flow of old water revisited at the hillslope scale?

J. Klaus et al.

Title Page

Abstract	Introduction
Conclusions	References
Tables	Figures

|◄ | ►|

◄ | ►

Back | Close

Full Screen / Esc

Printer-friendly Version

Interactive Discussion

Zehe, E., Elsenbeer, H., Lindenmaier, F., Schulz, K., and Blöschl, G.: Patterns of predictability in hydrological threshold systems, Water Resour. Res., 43, W07434, doi:10.1029/2006wr005589, 2007.

Macropore flow of old water revisited at the hillslope scale?

J. Klaus et al.

Title Page

Abstract | Introduction

Conclusions | References

Tables | Figures

|◀ | ▶|

◀ | ▶

Back | Close

Full Screen / Esc

Printer-friendly Version

Interactive Discussion

Table 1. Summary of irrigation for each experiment, duration (*D*), amount (*A*) and intensity (Int) for every irrigation block. Standard deviation is given for the precipitation sums in brackets.

	Block 1			Block 2			Block 3			Total
	D (min)	A (mm)	Int $(mm\,h^{-1})$	D (min)	A (mm)	Int $(mm\,h^{-1})$	D (min)	A (mm)	Int $(mm\,h^{-1})$	Sum (mm)
Experiment 1	80	12.3 (8.7)	9.3	60	11.9 (9.7)	11.9	80	9.7 (5.4)	7.28	33.9 (22.2)
Experiment 2	35	5.3 (2.3)	9.1	90	17.6 (8.9)	11.7	90	18.2 (8.9)	12.1	41.1 (18.6)
Experiment 3	90	18.1 (9.9)	12.1	90	21.8 (11.6)	14.5	–	–	–	39.9 (18.9)

Table 2. Pre-experimental conditions.

	45 day precipitation mm	10 day precipitation mm	45 day potential evaporation mm	10 day potential evaporation mm
Experiment 1	137	10.9	102.8	15.3
Experiment 2	43.3	9.2	146.2	24.1
Experiment 3	30.1	0	109.2	19.5

Table 3. Number of worm burrows with specific diameter (d) per square meter, measured at two plots for the first two experiments.

diameter	2–3 mm	3–5 mm	>5 mm	Total
Plot 1, Experiment 1	68	20	0	88
Plot 2, Experiment 1	40	8	1	49
Plot 1, Experiment 2	65	21	2	88
Plot 2, Experiment 2	90	19	1	110

Table 4. Results of the compartmental mixing modeling performed for every location, and for the two and three end member modeling. Soil depth is the center depth of a soil compartment (cm), PESW is the proportion of pre-event soil matrix water in the soil compartment (%), IW is the proportion of irrigation water in the soil compartment (%), OC is the proportion of water from the overlying cell (%), Error WB the error in the water balance (%), Error ^{2}H is the error in the mass balance of deuterium (%), and Error ^{18}O is the error in the mass balance of oxygen-18 (%).

Compartment	Soil depth (cm)	PESW	IW	OC	Error WB	Error ^{2}H	Error ^{18}O
Location 1, two components							
1	−15.5	76.29	23.71	–	−2.10	6.17	−3.52
2	−27.5	65.94	34.06	–	−0.64	1.70	−1.02
3	−37.5	77.96	22.04	–	−0.82	1.87	−1.00
4	−45.5	90.05	9.95	–	−1.88	4.04	−1.93
5	−50.5	74.42	25.58	–	−1.77	3.99	−1.99
Location 1, three components							
2	−27.5	66.59	33.36	0.05	−0.79	1.70	−0.92
3	−37.5	77.45	22.54	0.01	−0.76	1.85	−1.08
4	−45.5	90.12	9.88	0.00	−1.89	4.04	−1.92
5	−50.5	0.01	29.89	70.10	−1.76	3.87	−1.89
Location 2, two components							
1	−17.5	89.17	10.83	–	−2.05	5.04	−2.63
2	−27.5	85.48	14.52	–	−1.89	4.85	−2.62
3	−36.5	72.76	27.24	–	−1.53	3.29	−1.61
4	−44.5	63.43	36.57	–	−1.24	2.59	−1.25
5	−49.5	67.85	32.15	–	−1.24	2.14	−0.84
Location 2, three components							
2	−27.5	85.56	14.44	0.00	−1.90	4.85	−2.61
3	−36.5	74.07	25.89	0.04	−1.66	3.30	−1.45
4	−44.5	63.27	36.72	0.00	−1.23	2.59	−1.27
5	−49.5	66.76	33.24	0.01	−1.16	2.15	−0.94

Title Page

Abstract | Introduction

Conclusions | References

Tables | Figures

◀ | ▶

◀ | ▶

Back | Close

Full Screen / Esc

Printer-friendly Version

Interactive Discussion

Table 4. Continued.

Compartment	Soil depth (cm)	PESW	IW	OC	Error WB	Error ^{2}H	Error ^{18}O
		Location 3, two components					
1	−21.5	87.71	12.29	–	−0.43	1.28	−0.83
2	−29.5	94.26	5.74	–	0.54	−1.22	0.71
3	−39.5	59.34	40.66	–	−0.33	0.55	−0.21
4	−47.5	88.30	11.70	–	−1.30	1.43	−0.09
5	−54.5	100.00	0.00	–	0.18	2.02	−2.12
		Location 3, three components					
2	−29.5	34.76	20.31	44.93	−0.01	−0.08	0.09
3	−39.5	34.52	48.65	16.83	−0.50	1.19	−0.65
4	−47.5	95.72	4.20	0.09	−1.63	1.18	0.51
5	−54.5	32.89	0.00	67.11	−1.81	2.56	−0.66
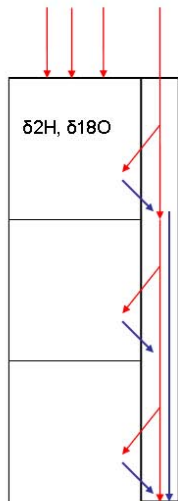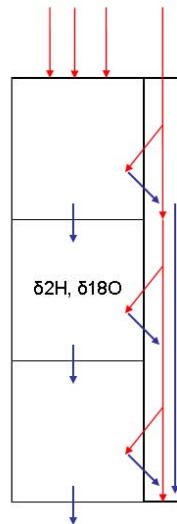
Fig. 1. Perceptual flow models for interaction of macropores and soil matrix compartments. Red arrows denote for the irrigation water, blue arrows denote for soil water. The boxes represent soil layers, while the continuous box represents a preferential flow path.
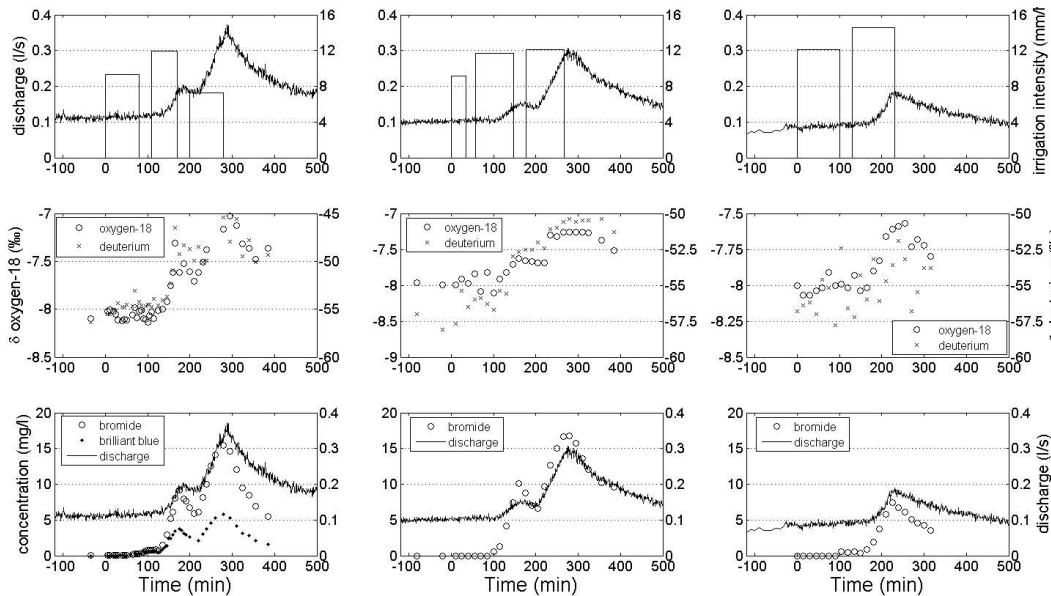
Fig. 2. Summary of the experiments, left column is experiment 1 (highest pre-experiment precipitation), center column experiment 2 (moderate pre-experiment precipitation), right column experiment 3 (lowest pre-experiment precipitation). Hydrographs, irrigation intensity, isotopic composition of tile drain water, bromide and brilliant blue concentrations are plotted.
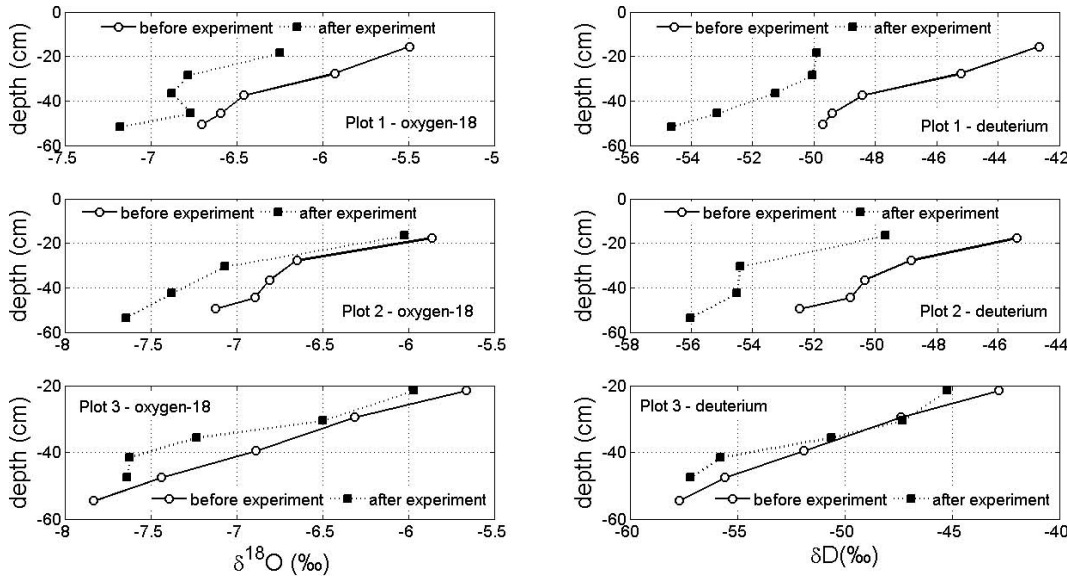
Fig. 3. Measured isotopic composition of soil water, before (blue) and after (red) the second experiment at three sampling locations. Left column summarizes oxygen-18 (VSMOW in ‰) and the right column summarizes deuterium (VSMOW in ‰).

Full Screen / Esc

Printer-friendly Version

Interactive Discussion
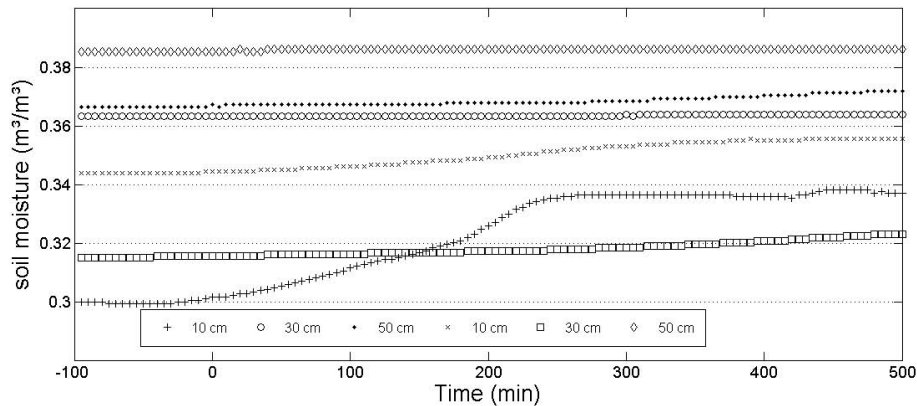
Fig. 4. Soil moisture dynamic during the second experiment, two theta probes for soil depths of 10 cm, 30 cm, and 50 cm, with a lateral distance of approximately 25 cm.
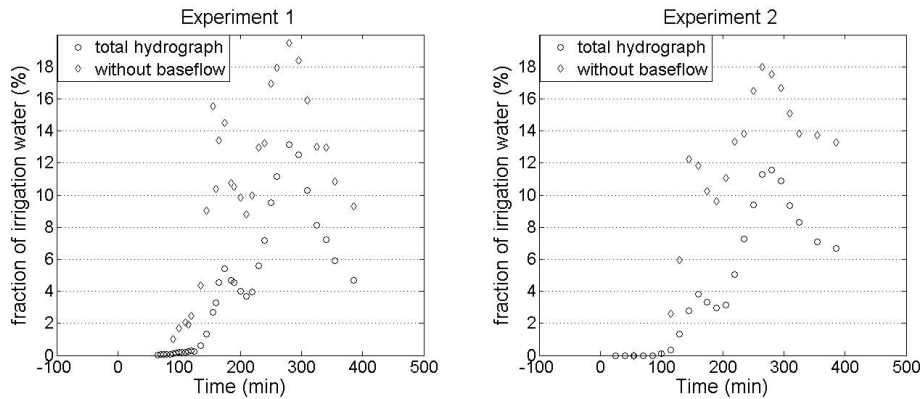
Fig. 5. Hydrograph separation of the first (left panel) and second (right panel) experiment. Shown is the proportion of irrigation water at the tile drain discharge in the total measured discharge, and with baseflow subtracted.
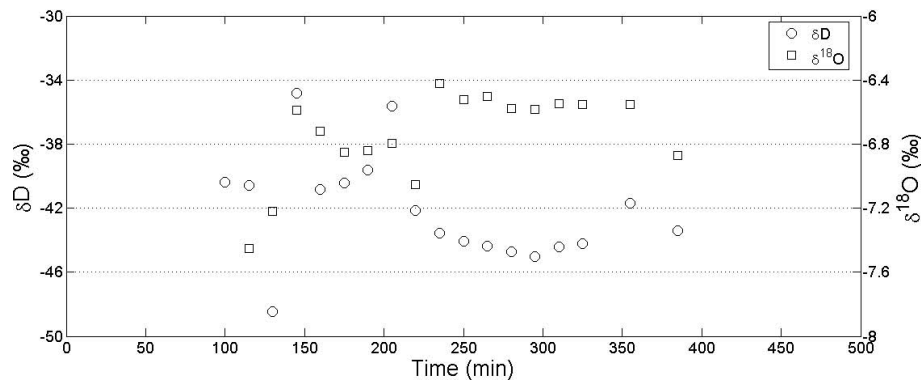
Fig. 6. Results from the backward hydrograph separation. The isotope values denote the isotopic composition of the soil water contributing to the tile drain discharge during the hydrograph of the second experiment.
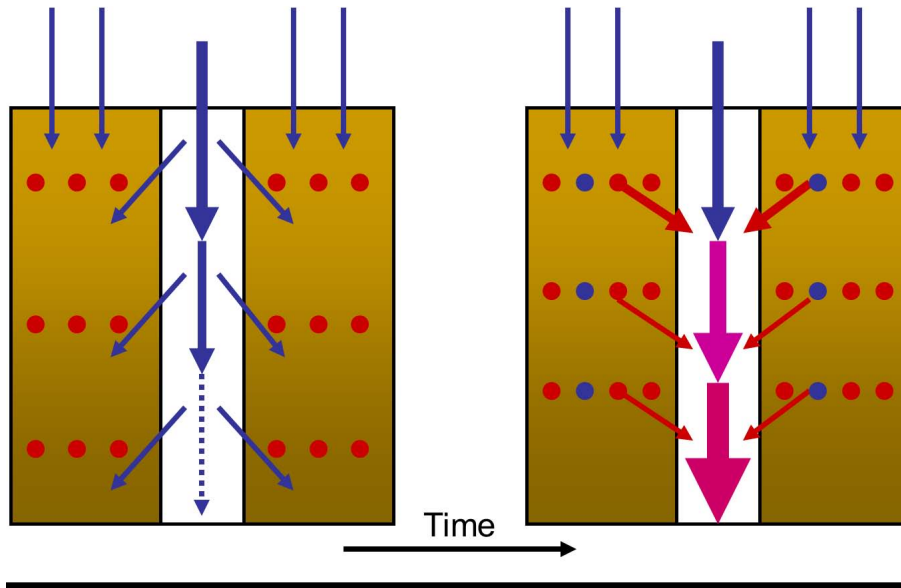
Fig. 7. Conceptual flow model of the field soil. Brown color indicates the soil matrix, the with box a preferential flow path. Red color indicates old water, blue color indicates new/irrigation water. Violet indicates mixed waters. At the beginning of the experiment (left panel) irrigation water infiltrates in the soil matrix at the surface and via macropores, only a small amount of irrigation water reaches the tile drain. With increasing storage in the system soil water enters the preferential flow paths and mixes there with irrigation water. Mostly old water reaches the tile drain.

Fig. 8. Correlation between hydrograph phases and isotopic composition of tile drain water. Left column are the results of the first experiment and the right column for the second experiment. Magenta denotes the isotopic composition of the irrigation water, light blue the isotopic composition of the rising hydrograph limb, dark blue the isotopic composition of the falling hydrograph limb, red the isotopic composition of baseflow conditions, and green the isotopic composition after the event.